Journal of Photochemistry and Photobiology A: Chemistry 213 (2010) 152–157

Contents lists available at ScienceDirect

Journal of Photochemistry and Photobiology A: Chemistry

journal homepage: www.elsevier.com/locate/jphotochem

A new class of organic dyes based on acenaphthopyrazine for dye-sensitized solar cells

Zhixia Kong [a], Huizhi Zhou [a], Jingnan Cui [a,*], Tingli Ma [a], Xichuan Yang [a], Licheng Sun [b,**]

[a] State Key Laboratory of Fine Chemicals, Dalian University of Technology (DUT), 158 Zhongshan Road, 116012 Dalian, China
[b] School of Chemical Science and Engineering, Center of Molecular Devices, Organic Chemistry, Royal Institute of Technology (KTH), Teknikringen 30, 10044 Stockholm, Sweden

ARTICLE INFO

Article history:
Received 24 August 2009
Received in revised form 11 March 2010
Accepted 25 May 2010
Available online 4 June 2010

Keywords:
Dye-sensitized solar cells
Acenaphthopyrazine derivatives
o-Dicarboxyl groups

ABSTRACT

A new class of organic dyes based on acenaphthopyrazine derivatives, containing pyrazine group as the electron acceptor and *o*-dicarboxyl acids as the anchoring groups were designed and synthesized for application in dye-sensitized solar cells (DSCs). These dyes have short synthesis routes and are easily adsorbed on the surface of TiO_2. Under illumination of simulated AM1.5 solar light (100 mW cm^{-2}), a total solar energy conversion efficiency (η) of 4.04% was obtained for the 3-(diphenylamino)acenaphtho[1,2-*b*] pyrazine-8,9-dicarboxylic acid (**AP-1**) in the preliminary tests, in comparison with the conventional **N719** dye (η = 7.05%) under the same conditions.

1. Introduction

Dye-sensitized solar cells (DSCs) have attracted much attention due to their capability to convert solar light into electricity with low material and production costs since 1991 [1]. The pursuit of highly efficient dyes has been one of the most active subjects in the development of DSCs. In recent years, much attention has been paid to the research of organic dyes as substitutes of noble metal complexes due to many advantages, such as diversity of molecular structures, simple synthesis as well as low cost and environmental issues. For these reasons, different kinds of organic dyes have been designed and synthesized, such as coumarin dyes [2–4], hemicyanine dyes [5–7], indoline dyes [8–10], triphenylamine dyes [11–13], phenothiazine dyes [14], porphyrine dyes [15] and merocyanine dyes [16]. Although some organic dyes are approaching the work efficiency of **N3**/**N719** dyes [17–20], the Ru dyes still represent the most efficient sensitizers in DSCs so far. Searching for more efficient organic dyes is still a challenging task. Therefore, it is necessary to design and synthesize a new type of organic dyes for DSCs. Here, we report a new class of organic dyes **AP** and **APQ** for DSCs based on acenaphthopyrazine chromophore and using larger conjugate system acenaphthene as a bridge group, pyrazine as electron-withdrawing group, and *o*-carboxyl acids as the anchoring groups. In most of reported organic dyes, cyanoacrylic acid or rhodanine acetic acid unit served as electron acceptor and the anchoring group. Our dyes are different from those dyes, and the anchoring groups can easily binding to the semiconductor surface simultaneously with a consequent improvement in the electronic coupling of the dye, because the *o*-dicarboxyl groups are placed in the same benzene ring and ortho position. In order to investigate the effect of space between anchoring and electron-withdrawing groups on the efficiency of DSCs, the space difference between the carboxyl and pyrazine groups by one benzene ring was designed in **AP** and **APQ** dyes. According to the most effective DSCs' dyes, a diphenylamine or N-alkyl as the electron donor was also used in the **AP** and **APQ** dyes. From the photophysical and photoelectrochemical measurements, we found that this new class of acenaphthopyrazine dyes showed moderate performance on DSCs' applications.

2. Experimental

All chemicals were purchased commercially and used without further purification except for 4,5-diaminophthalonitrile which was synthesized according to Ref. [21] and toluene which was distilled from CaH_2 and molecular sieves BaO.

2.1. Synthesis

There are four steps for the synthesis of acenaphthopyrazine dyes **AP** and **APQ** in a moderate yield as shown in Scheme 1. First, acenaphthylene-1,2-dione **1** was bromized, and the intermediates **3** were obtained *via* palladium-catalyzed aromatic C–N coupling reactions of **2** with diphenylamine or N-alkylphenylamines

* Corresponding author. Tel.: +86 411 39893872; fax: +86 411 83673488.
** Corresponding author. Tel.: +46 8 790 8127.
E-mail addresses: jncui@dlut.edu.cn (J. Cui), lichengs@kth.se (L. Sun).

1010-6030/$ – see front matter © 2010 Elsevier B.V. All rights reserved.
doi:10.1016/j.jphotochem.2010.05.017

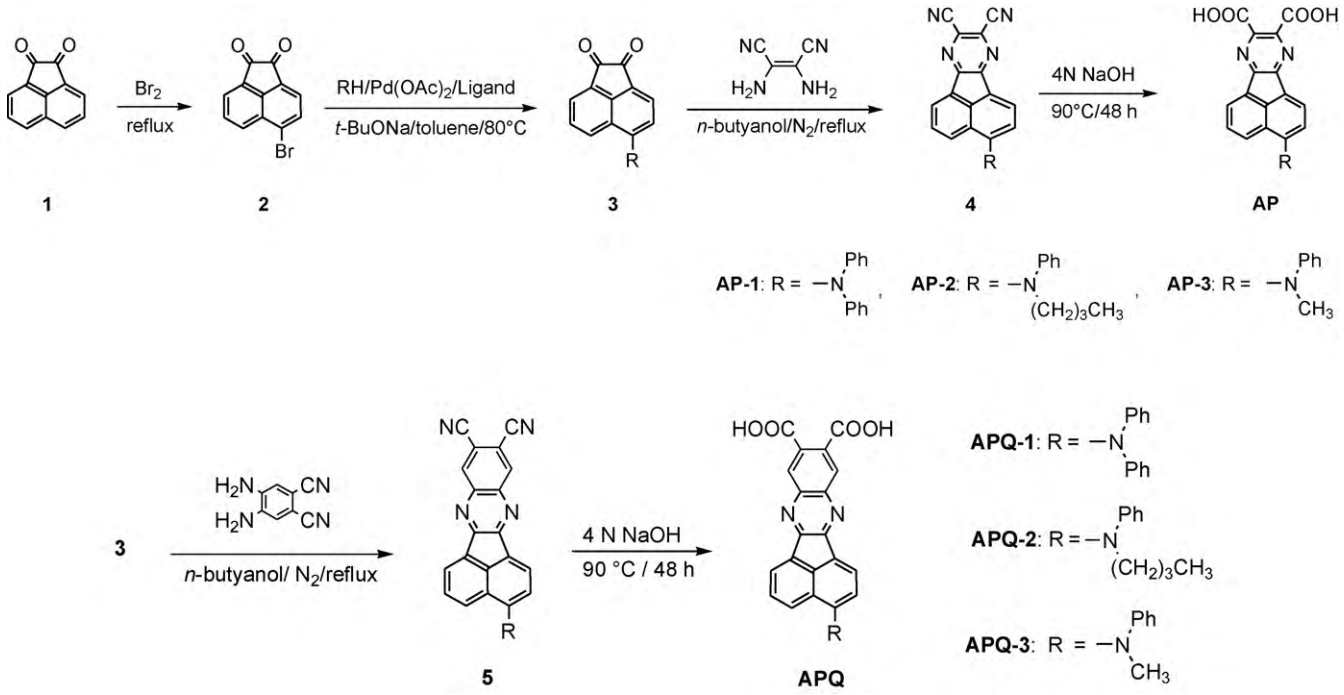

Scheme 1. Synthesis of **AP** and **APQ** dyes.

[22–24], then followed by the condensation of the dione **3** with 2,3-diaminomaleonitrile and 4,5-diaminophthalonitrile to obtain **4** and **5**, respectively. Finally, the acenaphthopyrazine dyes were obtained after hydrolysis of **4** and **5** in alkaline aqueous solution.

*2.1.1. 5-Bromoacenaphthylene-1,2-dione (**2**)*

A mixture of acenaphthene quinine **1** (20.0 g, 109.8 mmol) and liquid bromine (25.0 mL, 466.8 mmol) was stirred and refluxed for 2 h. The redundant bromine was removed by adding sodium bisulfite solution. Adding water into the reaction solution leads to the formation of a precipitate which was filtered, and repeatedly washed by water until pH reached 7.0 in filtrate. The crude product was purified by recrystallization in glacial acetic acid four times, and brown-yellow needle crystals were obtained (25.8 g, 90% yield). ^{1}H NMR (400 MHz, DMSO-d_6): δ 8.39 (d, J = 8.4 Hz, 1H), 8.21 (d, J = 7.6 Hz, 1H), 8.15 (d, J = 7.2 Hz, 1H), 8.04 (t, J = 7.6 Hz, 1H), 7.96 (d, J = 7.6 Hz, 1H); TOF HRMS EI+ m/z, calcd for $C_{12}H_6O_2$ 259.9473, found 259.9475.

*2.1.2. 5-(Diphenylamino)acenaphthylene-1,2-dione (**3-1**)*

This step was carried out under Ar with standard Schlenk techniques. A mixture of 5-bromo-acenaphthene quinone **2** (1000 mg, 3.84 mmol), diphenylamine (650 mg, 3.84 mmol), $Pd(OAc)_2$ (10 mg, 0.038 mmol), potassium *tert*-butanolate (520 mg, 4.60 mmol), and tri-*tert*-butylphosphonium tetrafluoroborate (30 mg, 0.1 mmol) in dry toluene (150 mL) was stirred at 80 °C under Ar till TLC monitoring indicated complete consumption of the amine. After cooling, the mixture was filtered. The filtrate was diluted with ether, and the organic phase was washed with water and brine, and dried over $MgSO_4$. After removing the organic solvent, the residue was purified by chromatography on a silica gel column using dichloromethane–petroleum ether (2/1, v/v) as an eluent to give a brown solid (353 mg, 26.4% yield). ^{1}H NMR (400 MHz, $CDCl_3$): δ 8.03 (d, J = 8.0 Hz, 1H), 7.97 (d, J = 6.8 Hz, 1H), 7.73 (d, J = 8.8 Hz, 1H), 7.49 (t, J = 7.8 Hz, 1H), 7.37 (d, J = 7.6 Hz, 1H), 7.32 (t, J = 7.6 Hz, 4H), 7.12 (m, 6H), MS APCI: $[M+H]^+$ (350.1, m/z).

*2.1.3. 3-(Diphenylamino)acenaphtho[1,2-b] pyrazine-8,9-dicarbonitrile (**4-1**) [25]*

A mixture of 2,3-diaminomaleonitrile (124 mg, 1.1 mmol) and **3-1** (400 mg, 1.1 mmol) in dry 1-butanol (10 mL) was refluxed for 4 h under N_2. The mixture was extracted with dichloromethane, the organic phase was washed with water and dried over $MgSO_4$. After removing the organic solvent, the residue was purified by chromatography on silica gel column using dichloromethane–petroleum ether (2/1, v/v) as an eluent to give a dark-red solid (325 mg, 88.5% yield). ^{1}H NMR (400 MHz, $CDCl_3$): δ 8.38 (d, J = 7.2 Hz, 1H), 8.30 (d, J = 8.0 Hz, 1H), 7.88 (d, J = 8.8 Hz, 1H), 7.58 (t, J = 7.8 Hz, 1H), 7.39 (d, J = 8.0 Hz, 1H), 7.34 (t, J = 7.8 Hz, 4H), 7.18 (m, 6H); TOF GCMS EI+ m/z, calcd for $C_{28}H_{15}N_5$ 421.1327, found 421.1330.

*2.1.4. 3-(Diphenylamino)acenaphtho[1,2-b] pyrazine-8,9-dicarboxylic acid (**AP-1**)*

A mixture of compound **4-1** (325 mg, 0.77 mmol) in 4 M aqueous solution of sodium hydroxide (60 mL) was stirred at 90 °C for 48 h. After cooling, the mixture was diluted with water. The precipitate was filtrated, washed with ether, then suspended in diluted hydrochloric acid solution for acidification, filtrated and red solid (250 mg, 70.6% yield) was obtained by filtration. ^{1}H NMR (400 MHz, DMSO-d_6): δ 8.37 (m, 2H), 7.81 (d, J = 8.4 Hz, 1H), 7.71 (t, J = 7.6 Hz, 1H), 7.36 (m, 5H), 7.13 (m, 6H); TOF HRMS ES− m/z, calcd for $C_{28}H_{16}N_3O_4$ 458.1141, found 458.1126.

*2.1.5. 3-(Butyl(phenyl)amino)acenaphtho[1,2-b] pyrazine-8,9-dicarboxylic acid (**AP-2**)*

The synthesis of **AP-2** dye was similar to **AP-1**. 81.9% yield; red solid; ^{1}H NMR (400 MHz, DMSO-d_6): δ 8.43 (d, J = 7.6 Hz, 1H), 8.34 (d, J = 6.8 Hz, 1H), 7.73 (d, J = 8.0 Hz, 1H), 7.70 (m, 2H), 7.26 (t, J = 7.8 Hz, 2H), 6.97 (m, 3H), 4.02 (t, J = 7.4 Hz, 2H), 1.70 (m, 2H), 1.41 (m, 2H), 0.89 (t, J = 7.4 Hz, 3H); TOF HRMS ES− m/z, calcd for $C_{26}H_{26}N_3O_4$ 438.1454, found 438.1443.

*2.1.6. 3-(Methyl(phenyl)amino)acenaphtho[1,2-b] pyrazine-8,9-dicarboxylic acid (**AP-3**)*

The synthesis of **AP-3** dye was similar to **AP-1**. 65.6% yield; orange-red solid; ^{1}H NMR (400 MHz, DMSO-d_6): δ 8.41 (d, J = 7.6 Hz, 1H), 8.34 (d, J = 6.8 Hz, 1H), 7.76 (d, J = 8.8 Hz, 1H), 7.67 (t, J = 7.6 Hz, 1H), 7.59 (d, J = 7.6 Hz, 1H), 7.30 (t, J = 7.6 Hz, 2H), 7.06 (d, J = 8.0 Hz, 2H), 7.01 (t, J = 7.4 Hz, 1H), 2.51 (s, 3H); TOF HRMS ES− m/z, calcd for $C_{23}H_{14}N_3O_4$ 396.0984, found 396.0972.

*2.1.7. 3-(Diphenylamino)acenaphtho[1,2-b]quinoxaline-9,10-dicarboxylic acid (**APQ-1**)*

The synthesis of **APQ-1** dye was similar to **AP-1**. 32.6% yield; red solid; ^{1}H NMR (400 MHz, DMSO-d_6): δ 8.40 (m, 3H), 7.80 (d, J = 8.4 Hz, 1H), 7.73 (t, J = 7.4 Hz, 1H), 7.44 (d, J = 8.0 Hz, 1H), 7.35 (t, J = 7.8 Hz, 4H), 7.47 (m, 6H); TOF HRMS ES− m/z, calcd for $C_{32}H_{18}N_3O_4$ 508.1297, found 508.1286.

*2.1.8. 3-(Butyl(phenyl)amino)acenaphtho[1,2-b]quinoxaline-9,10-dicarboxylic acid (**APQ-2**)*

The synthesis of **APQ-2** dye was similar to **AP-1**. 32.0% yield; orange-red solid; ^{1}H NMR (400 MHz, DMSO-d_6): δ 8.46 (m, 3H), 8.37 (d, J = 6.4 Hz, 1H), 7.73 (m, 3H), 7.25 (t, J = 8.0 Hz, 2H), 6.93 (m, 3H), 4.02 (t, J = 7.4 Hz, 2H), 1.70 (m, 2H), 1.41 (m, 2H), 0.90 (t, J = 7.4 Hz, 3H); TOF HRMS ES− m/z, calcd for $C_{30}H_{22}N_3O_4$ 488.1610, found 488.1613.

*2.1.9. 3-(Methyl(phenyl)amino)acenaphtho[1,2-b]quinoxaline-9,10-dicarboxylic acid (**APQ-3**)*

The synthesis of **APQ-3** dye was similar to **AP-1**. 50.3% yield; orange-red solid; ^{1}H NMR (400 MHz, DMSO-d_6): δ 8.95 (s, 1H), 8.94 (s, 1H), 8.46 (d, J = 7.2 Hz, 1H), 8.39 (d, J = 6.4 Hz, 1H), 7.78 (d, J = 8.4 Hz, 1H), 7.11 (t, J = 7.6 Hz, 1H), 7.65 (d, J = 7.2 Hz, 1H), 7.27 (t, J = 7.6 Hz, 2H), 7.11 (m, 3H), 3.58 (s, 3H); TOF HRMS ES− m/z, calcd for $C_{27}H_{16}N_3O_4$ 446.1141, found 446.1145.

2.2. Fabrication of the nanocrystalline TiO_2 solar cells

Titania paste from Solaronix-D (Solaronix, Switzerland) [17] was deposited onto the conducting glass by doctor blading, with the 12 μm film thickness, 0.2 cm^2 active area. The photoelectrode was sintered at 500 °C for 30 min in air and cooled to room temperature. For the dye uptake, the electrode was immersed into the dye solutions [5×10^{-4} M in a mixture of acetonitrile and *tert*-butyl alcohol (v/v, 1:1)], and kept at room temperature for 10 h, then rinsed with EtOH and dried. A platinized counter electrode was clipped onto the top of the TiO_2 working electrode and electrolyte solution was added between the two electrodes *via* capillary action. The electrolyte was composed of 0.06 M lithium iodide, 0.60 M 1,2-dimethyl-3-propylimidazolinium iodine (DMPII), 0.03 M I_2, 0.5 M 4-*tert*-butylpyridine (TBP) and 0.10 M GuSCN in acetonitrile.

2.3. Characterization of the dyes

^{1}H NMR spectra were measured with VARIAN INOVA400 MHz (USA) with the chemical shifts against TMS. Mass spectra were measured on an HP 1100 LC-MSD spectrometer, and high-resolution mass spectra (HRMS) were obtained on HPLC-Q-Tof MS (Micro) spectrometer. Absorption and emission spectra were recorded with HP8453 (USA) and PTI700 (USA), respectively. Electrochemistry was measured with BAS100W (USA). IR spectra were measured with 20DXB. The geometrical and electronic properties of the dyes were studied with DFT calculations using Gaussian 03 program package.

2.4. Photocurrent–voltage measurements

The irradiation source for the photocurrent–voltage (J–V) measurement was an AM 1.5 solar simulator (16S-002, Solar Light Co. Ltd., USA). The incident light intensity was 100 mW cm^{-2} calibrated with a standard silicon solar cell. The current–voltage curves were obtained by linear sweep voltammetry (LSV) method using an electrochemical workstation (LK9805, Lanlike Co. Ltd., China). The measurement of the incident photon-to-current conversion efficiency (IPCE) was performed by a Hypermonolight (SM-25, Jasco Co. Ltd., Japan).

3. Results and discussion

3.1. Photophysical and electrochemical properties

The absorption spectra of the dyes in the mixture of acetonitrile (**AN**) and *tert*-butyl alcohol (v:v = 1:1, *t*-BuOH-AN) are displayed in Fig. 1 and the data are listed in Table 1. The absorption maxima of 461, 457, and 444 nm were obtained for **AP-1**, **-2** and **-3** dyes, while the **APQ-1**, **-2** and **-3** dyes showed 444, 435, 424 nm in the solution, respectively. Compared with the absorptions, λ_{max} of **AP** is red-shifted than **APQ** dyes, indicating stronger electron push–pull system in **AP** dyes than **APQ** dyes, although **APQ** dyes have bigger conjugate system than **AP** dyes. The bigger conjugate system in **APQ** dyes show higher extinction coefficients ε than **AP** dyes. When the dyes were attached to TiO_2, the absorption maxima of these dyes were blue-shifted by 0, 6, 3, 8, 7, and 3 nm for **AP-1**, **-2**, **-3**, **APQ-1**, **-2** and **-3**, respectively. The deprotonation of carboxylic acid in the dye molecule [19] and possible aggregation upon adsorption on the TiO_2 film, as discussed in the following IR analysis, may contribute to this blue-shift. The aggregation of **AP-1** dye in *t*-BuOH-AN

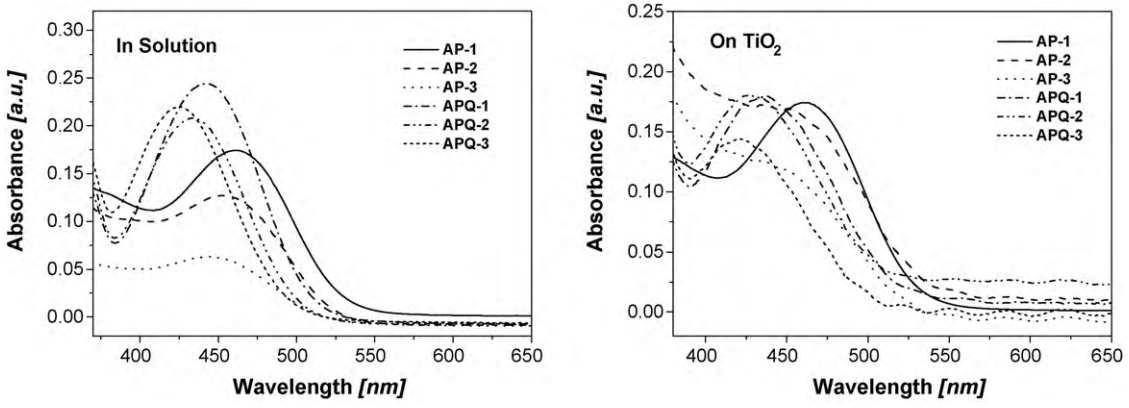

Fig. 1. Absorption spectra of acenaphthopyrazine dyes in *t*-BuOH-AN solution (left) and on TiO_2 films (right).

Table 1
Absorption, emission, electrochemical properties of the acenaphthopyrazine dyes.

Dye	Absorption[a]			Emission[a]	Oxidation potential		
	λ_{max} (nm)	ε at λ_{max} ($M^{-1}\,cm^{-1}$)	λ_{max} on TiO_2 [b] (nm)	λ_{max} (nm)	E_{ox} (V) (versus NHE)[c]	E_{0-0} (V) (Abs/Em)[d]	E_{ox-0-0} (V) (versus NHE)
AP-1	461	0.87×10^4	461	603	1.33	2.17	−0.84
AP-2	457	0.63×10^4	451	599	1.28	2.31	−1.03
AP-3	444	0.31×10^4	441	585	1.25	2.32	−1.07
APQ-1	444	1.22×10^4	436	590	1.31	2.35	−1.04
APQ-2	435	1.04×10^4	428	608	1.26	2.39	−1.13
APQ-3	424	1.10×10^4	421	607	1.21	2.45	−1.24

[a] Absorption and emission spectra were measured in *t*-BuOH-AN solution (2×10^{-5} M) at room temperature.
[b] Absorption spectra on TiO_2 were obtained through measuring the dye adsorbed on TiO_2 film in *t*-BuOH-AN.
[c] The electrochemical properties were measured in acetonitrile with 0.1 M *tetra*-butylammonium hexafluorophosphate ($TBAPF_6$) as supporting electrolyte (working electrode: glassy carbon; reference electrode: Ag/Ag^+; calibrated with ferrocene/ferrocenium (Fe/Fe^+) as an internal reference and converted to NHE by addition of 630 mV; counter electrode: Pt).
[d] The E_{0-0} was estimated from the intersection between the absorption and emission spectra.

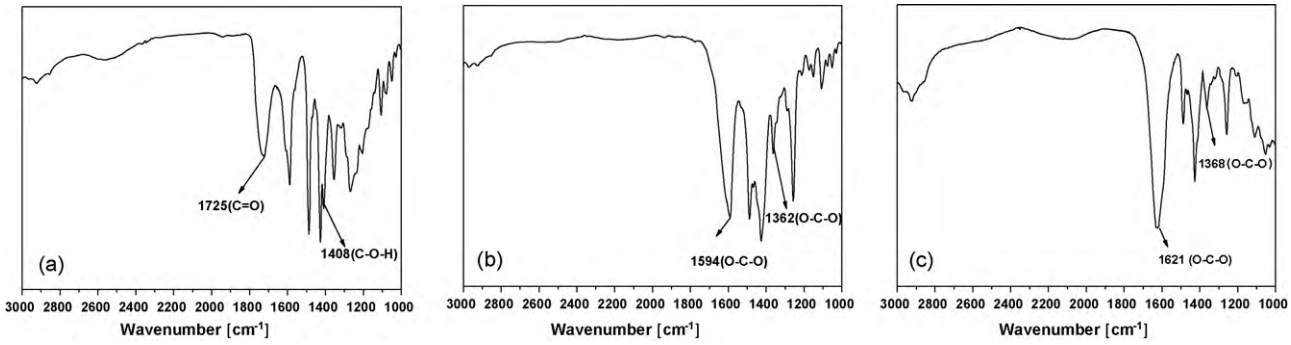

Fig. 2. FT-IR spectra for dye **AP-1** (a), sodium salt of **AP-1** (b) and adsorbed on TiO_2 film (c).

was not been observed by increasing concentration of the dye from 1.0×10^{-5} to 2.0×10^{-4} M.

Cyclic voltammetry (CV) was employed to measure the electrochemical properties of these dyes and the results are shown in Table 1. The first oxidation potential (E_{ox}) corresponds to the HOMO level of the dye. From the data in Table 1, it is known that the HOMO levels of the dyes are sufficiently more positive than I^-/I_3^- redox couple, indicating that the oxidized dyes could be reduced effectively by electrolyte and then regenerated. The LUMO levels of these dyes were calculated by E_{ox}–E_{0-0}, where E_{0-0} is the zeroth–zeroth energy of the dyes estimated from the intersection between the absorption and emission spectra, and the data are listed in Table 1. To effectively inject the electron into the conducing band (CB) of TiO_2, the LUMO levels of the dyes must be sufficiently more negative than the conducing band energy (E_{cb}) of semiconductor, −0.5 V (versus NHE) [26]. From the LUMO values, we can find that all of acenaphthopyrazine dyes can complete the process of electron injection into CB of TiO_2 to form the oxidized dyes.

3.2. Binding mode of dye molecules to the TiO_2 surface

In order to determine the detailed structure of acenaphthopyrazine dyes adsorbed on the TiO_2 surface, which is associated with the interfacial electron injection, FT-IR absorption for **AP-1** powder, sodium salt of **AP-1** and TiO_2 films exposed to **AP-1** solution was measured, and the spectra are shown in Fig. 2. For the dye powder, the 1725 cm^{-1} peak is assigned to carbonyl group in the carboxylic acid. The peak at 1408 cm^{-1} results from the in-plane bending of C–O–H. After the dye was adsorbed onto the TiO_2 surface, the peak, diagnostic of –COOH at 1725 and 1408 cm^{-1} disappeared, while asymmetric and symmetric peaks for $–COO^-$ group were observed, respectively, at 1621 and 1368 cm^{-1}, owing to the deprotonation of carboxylic acid upon dye adsorption and lead to the blue-shift of the absorption, indicating the two carboxyl groups bind to the TiO_2 surface simultaneously. The separation between the asymmetric and symmetric peak for $–COO^-$ is calculated to be 253 cm^{-1}, comparable to that (232 cm^{-1}) for the solid salt form, indicating a bidentate coordination mode of the dye to the TiO_2 surface [27].

3.3. Photovoltaic performance of DSCs

The data for photovoltaic performance are shown in Table 2 and *J–V* curves of the dyes are shown in Fig. 3 (left). The highest value of conversion efficiency (η) among these dyes was 4.04% for the **AP-1** in the preliminary tests, under the same conditions, the efficiency of **N719** was 7.05%. Similar to triphenylamine dyes [11–13], the efficiency of **AP-1** and **APQ-1** dyes was higher than the other dyes, which can be ascribed to the bigger conjugate system. The incident photon-to-current conversion efficiencies (IPCEs) of these dyes in DSCs are shown in Fig. 3 (right), which is in agreement

Table 2
Photovoltaic performance of acenaphthopyrazine dyes.[a].

Dye[b]	J_{SC} ($mA\,cm^{-2}$)	V_{OC} (mV)	Fill factor (ff)	η (%)
AP-1	8.11	693	0.719	4.04
AP-2	6.43	662	0.630	2.68
AP-3	4.10	638	0.697	1.82
APQ-1	6.27	650	0.699	2.85
APQ-2	5.89	632	0.705	2.62
APQ-3	3.78	589	0.663	1.48
N719	13.09	820	0.657	7.05

[a] The photovoltaic performance of acenaphthopyrazine dyes was measured under irradiation of AM 1.5 G simulated solar light (100 mW cm^{-2}) at room temperature, 12 μm film thickness which adopted Solaronix-D titania paste, 0.2 cm^2 working area.
[b] The concentration of dyes is 5×10^{-4} M in a mixture of acetonitrile and *tert*-butyl alcohol (v/v, 1:1), 0.6 M DMPII, 0.03 M I_2, 0.1 M GuSCN, 0.5 M TBP, and 0.06 M LiI in acetonitrile as electrolyte.

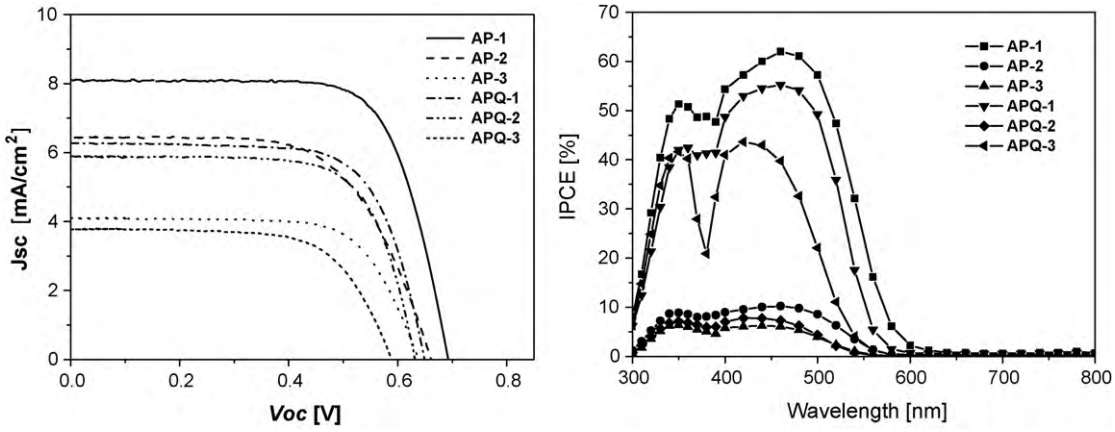

Fig. 3. *J–V* curves (left) and IPCE spectra (right) of DSCs based on acenaphthopyrazine dyes.

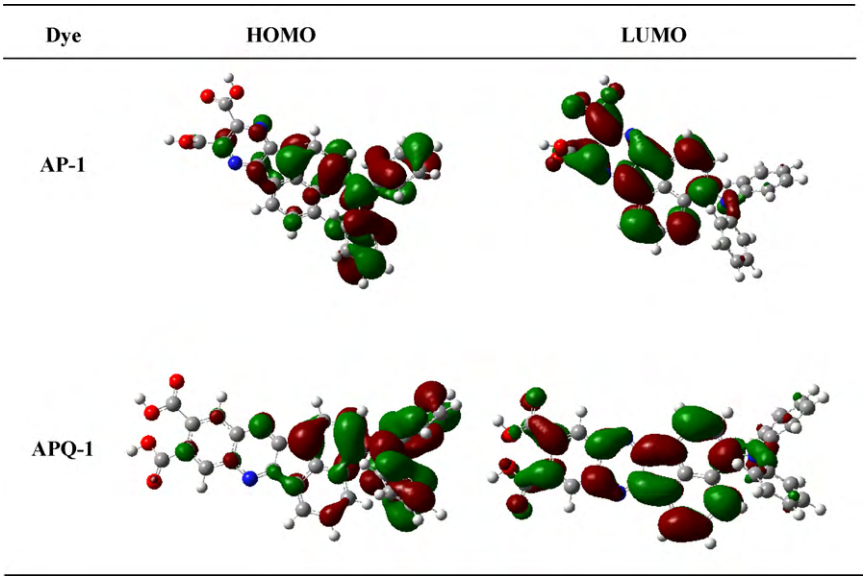

Fig. 4. The frontier orbitals of the **AP-1** and **APQ-1** dyes optimized at the B3LYP/6-31+G(d) level and B3LYP/3-21+G, respectively.

with the absorption spectra of the dyes. The highest value obtained for **AP-1** was 63% at 460 nm. It seems that introduction of long-wavelength chromophore to **AP** dyes may broaden the spectrum of absorption to get better IPCE. Compared to using **APQ** dyes, the photovoltaic performance of DSCs using **AP** dyes is better despite of **APQ** dyes have higher ε, indicating the space between anchoring and electron-withdrawing groups is an important factor and the small space is propitious to obtain the higher conversion efficiency.

3.4. Theoretical study of dye structure and electron distribution

In order to get a further insight into the difference in performance of DSCs based on these dyes, density functional theory (DFT) calculations [28] were performed for the geometry optimization. Fig. 4 shows the frontier molecular orbitals of **AP-1** and **APQ-1**. At the HOMO of the dye, the electron density is mainly distributed in the diphenylamine electron donor moiety, and with electronic excitation at the LUMO level, intramolecular charge transfer induced electron movement from the donor site to the acceptor moiety of the dye. The better photovoltaic performance of **AP-1** than **APQ-1** indicates that the space between *o*-dicarboxyl groups and acenaphthopyrazine in **AP-1** or **APQ-1** is important and excited electrons of **AP-1** can easily inject into the conduction band of TiO_2 *via* the *o*-dicarboxyl groups.

4. Summary

We have designed and synthesized a new class of organic dyes with acenaphthopyrazine chromophore containing larger conjugate system acenaphthene as a bridge group, pyrazine as electron-withdrawing group, and *o*-dicarboxyl acids as the anchoring groups. DSCs based on these dyes were prepared with nanostructured TiO_2. The **AP-1** dye has the highest efficiency (η = 4.04%) among these dyes in the preliminary tests, in comparison with **N719** dye (η = 7.05%) under the same conditions. The small space between anchoring and electron-withdrawing groups could be propitious to obtain the better photovoltaic performance of DSCs. By further structural modification of the acenaphthopyrazine dyes and optimization of test conditions, we expect to get even better DSC performance and related work is in progress.

Acknowledgments

We are grateful to the National Natural Science Foundation of China (90713030; 20876025), the National Basic Research Program of China (Grant No. 2009CB220009), the Program for Changjiang Scholars and Innovative Research Team in University (IRT0711), the Swedish Energy Agency, the Swedish Research Council, and the K & A Wallenberg Foundation for financial support of this work.

References

[1] B. O'Regan, M. Grätzel, Nature 353 (1991) 737–740.
[2] K. Hara, K. Sayama, Y. Ohga, A. Shinpo, S. Suga, H. Arakawa, Chem. Commun. (2001) 569–570.
[3] K. Hara, Z.S. Wang, T. Sato, A. Furube, R. Katoh, H. Sugihara, Y. Dan-oh, C. Kasada, A. Shinpo, S. Suga, J. Phys. Chem. B 109 (2005) 15476–15482.
[4] Z.-S. Wang, Y. Cui, Y. Dan-oh, C. Kasada, A. Shinpo, K.J. Hara, Phys. Chem. C 111 (2007) 7224–7230.
[5] Z.-S. Wang, F.-Y. Li, C.-H. Huang, Chem. Commun. (2000) 2063–2064.
[6] Z.-S. Wang, F.-Y. Li, C.-H. Huang, J. Phys. Chem. B 105 (2001) 9210–9217.
[7] Q.-H. Yao, F.-S. Meng, F.-Y. Li, H. Tian, C.-H. Huang, J. Mater. Chem. 13 (2003) 1048–1053.
[8] T. Horiuchi, H. Miura, K. Sumioka, S. Uchida, J. Am. Chem. Soc. 126 (2004) 12218–12219.
[9] S. Ito, S.M. Zakeeruddin, R. Humphry-Baker, P. Liska, R. Charvet, P. Comte, M.K. Nazeeruddin, P. Pe'chy, M. Takata, H. Miura, S. Uchida, M. Grätzel, Adv. Mater. 18 (2006) 1202–1205.
[10] S. Ito, H. Miura, S. Uchida, M. Takata, K. Sumioka, P. Liska, P. Comte, P. Pe'chy, M. Grätzel, Chem. Commun. (2008) 5194–5196.
[11] M. Velusamy, K.R.J. Thomas, J.T. Lin, Y.-C. Hsu, K.-C. Ho, Org. Lett. 7 (2005) 1899–1902.
[12] T. Kitamura, M. Ikeda, K. Shigaki, T. Inoue, N. Anderson, X. Ai, T. Lian, S. Yanagida, Chem. Mater. 16 (2004) 1806–1812.
[13] D.P. Hagberg, T. Edvinsson, T. Marinado, G. Boschloo, A. Hagfeldt, L. Sun, Chem. Commun. (2006) 2245–2247.
[14] H. Tian, X. Yang, R. Chen, Y. Pan, L. Li, A. Hagfeldt, L. Sun, Chem. Commun. (2007) 3741–3743.
[15] W.M. Campbell, K.W. Jolley, P. Wagner, K. Wagner, P.J. Walsh, K.C. Gordon, L. Schmidt-Mende, M.K. Nazeeruddin, Q. Wang, M. Grätzel, D.L. Officer, J. Phys. Chem. C 11 (2007) 11760–11762.
[16] K. Sayama, K. Hara, N. Mori, M. Satsuki, S. Suga, S. Tsukagoshi, Y. Abe, H. Sugihara, H. Arakawa, Chem. Commun. (2000) 1173–1174.
[17] M.K. Nazeeruddin, A. Kay, I. Rodicio, R. Humphry-Baker, E. Muller, P. Liska, N. Vlachopoulos, M. Grätzel, J. Am. Chem. Soc. 115 (1993) 6382–6390.
[18] M.K. Nazeeruddin, S.M. Zakeeruddin, R. Humphry-Baker, M. Jirousek, P. Liska, N. Vlachopoulos, V. Shklover, C.H. Fischer, M. Grätzel, Inorg. Chem. 38 (1999) 6298–6305.
[19] M.K. Nazeeruddin, P. Péchy, T. Renouard, S.M. Zakeeruddin, R. Humphry-Baker, P. Comte, P. Liska, L. Cevey, E. Costa, V. Shklover, L. Spiccia, G.B. Deacon, C.A. Bignozzi, M. Grätzel, J. Am. Chem. Soc. 123 (2001) 1613–1624.
[20] M.K. Nazeeruddin, F.D. Angelis, S. Fantacci, A. Selloni, G. Viscardi, P. Liska, S. Ito, B. Takeru, M. Grätzel, J. Am. Chem. Soc. 127 (2005) 16835–16847.
[21] W.J. Youngblood, J. Org. Chem. 71 (2006) 3345–3356.
[22] M. Nishiyama, T. Yamamoto, Y. Koie, Tetrahedron Lett. 39 (1998) 617–620.
[23] J.F. Hartwig, Angew. Chem. Int. Ed. 37 (1998) 2046–2067.
[24] J.F. Hartwig, Synlett (1997) 329–340.
[25] T.-H. Huang, J.T. Lin, Chem. Mater. 16 (2004) 5387–5393.
[26] A. Hagfeldt, M. Grätzel, Chem. Rev. 95 (1995) 49–68.
[27] G.B. Deacon, R.J. Phillips, Coord. Chem. Rev. 33 (1980) 227–250.
[28] M.J. Frisch, et al., Gaussian 03, Revision C.02, Gaussian, Inc., Wallingford, CT, 2004.